The Journal of Global Radiology

ENSURING MEDICAL IMAGING ACCESS FOR ALL

PICTORIAL ESSAY

Hand Manifestations of Systemic Diseases: Radiographic Imaging Findings and Approaches

Shweta Raviraj Poojary[1], Sujith Shekar[2], Hagalahalli Nagarajegowda Pradeep[2], Chakenahalli Puttaraj Nanjaraj[2], Prathibha PS[2]

1. Assistant Professor, Department of Radiology, JSS Medical College, Mysore.
2. Department of Radiology, Mysore Medical College and Research Institute, Mysore.

* **Corresponding author.** Current address: Dr. Shweta Poojary, shwetapoojary113@gmail.com

DOI: 10.7191/jgr.675

Published: March 5, 2024

Citation: Poojary et al. Hand Manifestations in Systemic Diseases: Radiographic Imaging Findings and Approaches. J Glob Radiol. 2024;10(1):675.

Keywords: Hand, X-ray, Disease

Word count: 3,293

Abstract

The hands act as a mirror in many systemic diseases. Identification of a variety of inflammatory, degenerative, congenital, and hematological diseases can be performed by a single hand radiograph which may help start early intervention and prevent morbidity. Endocrinological and metabolic disorders also may demonstrate signs on a hand radiograph. Granulomatous conditions and systemic connective tissue disorders demonstrate characteristic imaging features which may aid the diagnosis. Radiologists should be familiar with the radiographic imaging findings of common systemic disorders because these may be a problem solving tool to aid in diagnosis.

Introduction

The human hand is comprised of skin, bones, muscles, tendons, ligaments, nerves, and blood vessels. Although a very small part of the human body, it serves as an aid for reflecting the various manifestations of systemic diseases. The first ever X-Ray was that of the hand of Anna Bertha Roentgen, way back on November 15th, 1895 (1). In the current scenario, a review of a single hand radiograph has aided in the diagnosis of a wide range of metabolic, hematological, granulomatous, autoimmune, and congenital diseases. In some systemic diseases, the pathological changes of hand involvement may be an eye-opening initial presenting feature. The objective of this article is to highlight the importance of hand radiographs and to illustrate the typical radiological appearances of a wide selection of systemic disorders that may present on a radiograph of the hand. Table 1 highlights the spectrum of systemic disorders affecting hands.

ISSN 2372-8418

Table 1. The spectrum of systemic disorders that affect hands.

Disease Category	Subtypes
Arthritis	Osteoarthritis Rheumatoid arthritis Calcium pyrophosphate dihydrate (CPPD) deposition disease Psoriatic arthritis Gout Hypertrophic osteoarthropathy
Systemic connective tissue disorders and Granulomatous conditions	Scleroderma Dermatomyositis Marfan's syndrome Sarcoidosis Tuberculous dactylitis
Endocrine and Metabolic disorders	Thyroid acropachy Acromegaly Hypothyroidism Parathyroid disorders Hyperparathyroidism Hypoparathyroidism Pseudohypoparathyroidism Pseudo pseudo hypoparathyroidism Osteoporosis Rickets and osteomalacia Renal osteodystrophy Hemochromatosis
Hematologic disorders	Sickle cell disease Thalassemia Fanconi's Anemia Myelofibrosis Leukemia Hemophilia
Skeletal dysplasias	Mucopolysaccharidosis Achondroplasia Pyknodysostosis Osteopetrosis

Background

Arthritis

Inflammatory and degenerative arthritis account for the majority of arthritis cases. Both the conditions have different treatment options, so distinguishing between the two is essential. Charts 1 and 2 provide a systematic approach for arthritis diagnosis.

Osteoarthritis: Degenerative joint disease is the most common form of arthritis. Usually it is seen in the distal interphalangeal, first carpo-metacarpal, and scaphotrapezial joints. The proximal interphalangeal joints may occasionally be affected. Key radiographic features include asymmetric joint space narrowing, subchondral sclerosis, and osteophytes formation (Figure 1) (2).

Rheumatoid arthritis: Bilateral and symmetrical polyarthropathy (involvement of >3 joints) occurs in rheumatoid arthritis affecting metacarpophalangeal, proximal interphalangeal, midcarpal, radiocarpal, and distal radioulnar joints, with predilection for the ulnar styloid process. Radiographic findings include synovial swelling initially, which is followed by symmetric joint space

Figure 1. 60-year-old man with a history of joint pain, instability, and stiffness of hands. Posteroanterior radiograph of hand shows asymmetric joint space narrowing involving distal interphalangeal joints with subchondral sclerosis and osteophytes.

Chart 1. This chart illustrates an algorithm used to help establish the diagnosis of arthritis. The common joints of involvement are shown in star figures. CPPD = calcium pyrophosphate dehydrate deposition.

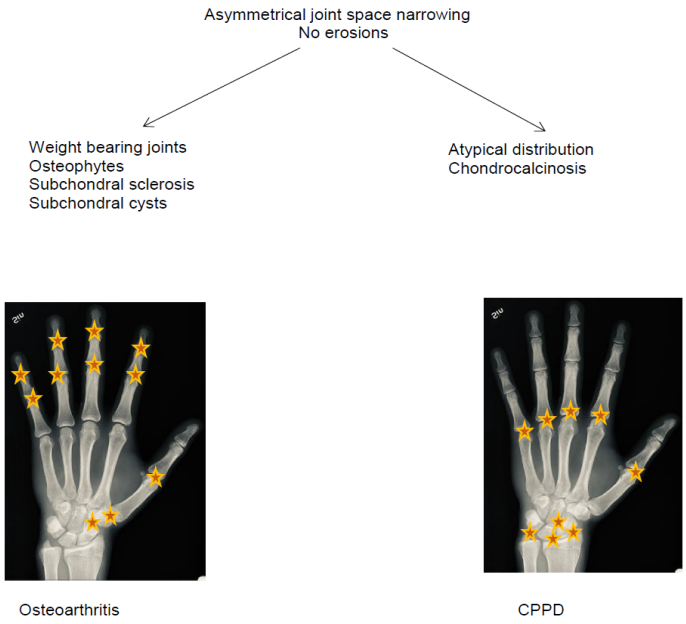

Chart 2. This chart illustrates an algorithm used to help establish the diagnosis of arthritis. The common joints of involvement are shown in star figures.

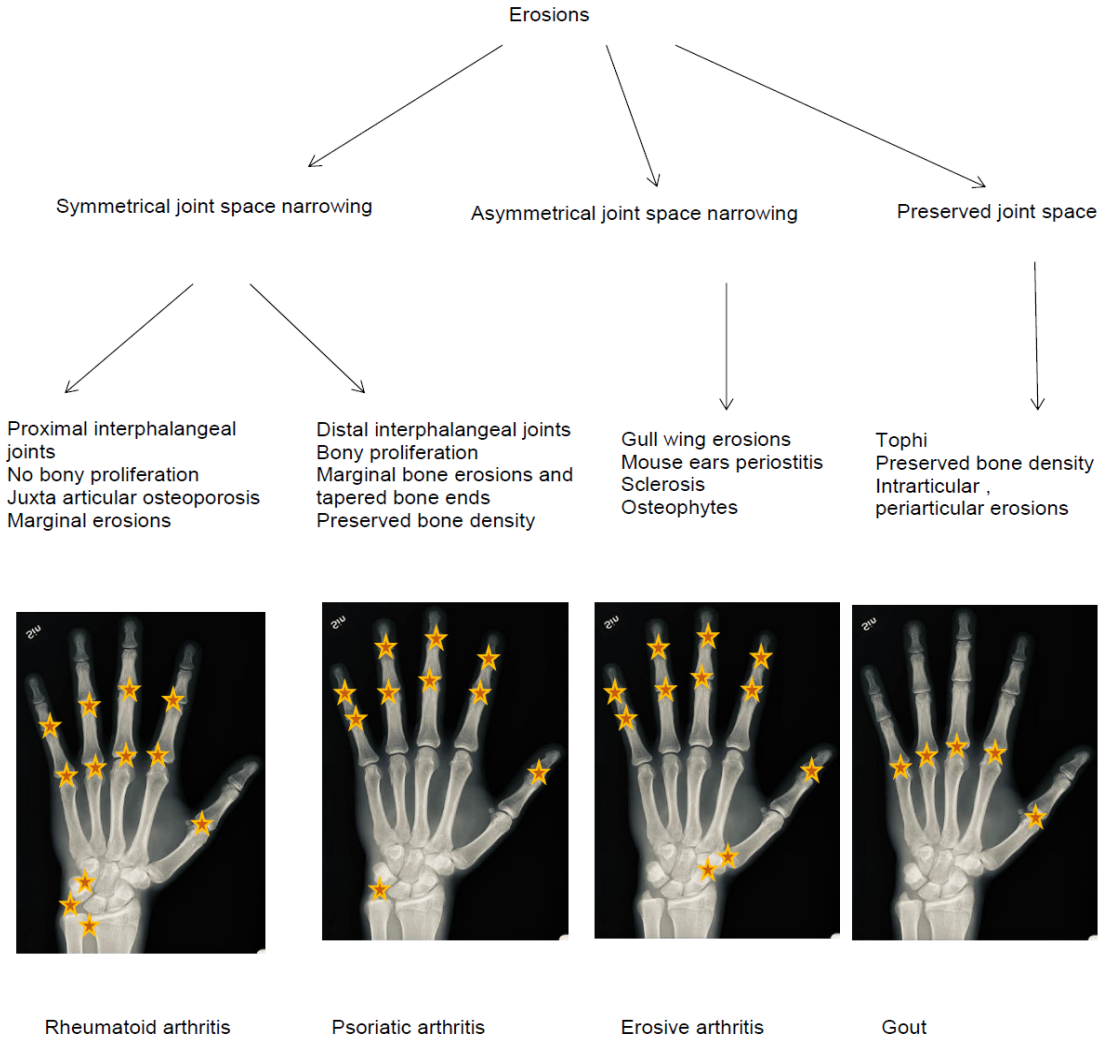

Figure 2. Rheumatoid arthritis in a 55-year-old female presenting with pain and deformity of the hands. Posteroanterior radiograph of both hands shows bilateral symmetric joint space narrowing involving metacarpophalangeal, interphalangeal, carpometacarpal, inter-carpal, radiocarpal, and distal radioulnar joints with periarticular osteopenia and bone erosions. Bony ankylosis of carpometacarpal and inter-carpal joints. Ulnar deviation of proximal phalanx of right fifth digit.

narrowing, peri-articular bone erosions and peri-articular osteopenia. Eventually, joint subluxation, contractures and deformities occur (Figure 2) (3).

CPPD deposition disease: Imaging findings in this disease are those of osteoarthritis with symmetric and unusual distribution involving non-weight-bearing joints such as the Radiocarpal joint of wrist, metacarpo-phalangeal joint, shoulder and elbow joint. Chondrocalcinosis occurs in the triangular fibrocartilage complex and luno-triquetral ligaments in the wrist. Large subchondral cysts are also seen (4).

Psoriatic arthritis: This is a common seronegative spondyloarthropathy with bone proliferation, enthesitis, and periostitis involving the distal joints of the hands and feet. Erosions tend to occur at the margins of the distal interphalangeal joints causing the "pencil in cup" appearance. Bilateral and asymmetrical involvement is seen with preserved bone density (Figure 3). Soft tissue swelling giving rise to the typical "sausage digit" appearance. Occasionally, acroosteolysis of the distal phalanx with soft tissue swelling and periostitis giving a sausage digit appearance is also observed (3).

Gout: Gout is a crystal deposition arthropathy caused by the deposition of monosodium urate crystals (tophi) in and around the joints. Acute phase presents with soft tissue swelling and joint effusion whereas the chronic tophaceous phase has asymmetrical articular, juxta-articular, or periarticular soft tissue nodular tophi. Bony erosions may be intra-articular,- peri-articular or distinct from the joint with 'punched out' in appearance with sclerotic and overhanging margins resembling rat bites (Figure 4). Bone density is preserved until late in the disease (5).

Hypertrophic osteoarthropathy: Hypertrophic osteoarthropathy can be a primary entity, known as pachydermoperiostosis, or secondary to pulmonary, pleural,

Figure 3. 55-year-old female with a long-standing history of psoriatic arthritis. Posteroanterior radiograph of hand shows joint space narrowing involving distal and proximal interphalangeal joints with bony erosions and 'pencil and cup' appearance in the distal interphalangeal joints.

Figure 4. Gout in a 40-year-old male presenting with swelling of the second digit. Postero-anterior radiograph of right hand shows soft tissue density nodular tophi involving the distal interphalangeal joint of 2nd digit with periarticular bony erosions.

mediastinal, and cardiovascular causes, as well as extra thoracic conditions such as gastrointestinal tumors and infections, cirrhosis, and inflammatory bowel disease. The most common of the hypertrophic osteo-arthropathies is hypertrophic pulmonary osteoarthropathy, a paraneoplastic syndrome secondary to carcinoma of the lung. The most common site of skeletal involvement is in the radius and ulna (80%). In the hands, a bilateral, symmetrical polyarthropathy is seen with proximal phalangeal periostosis (60%) and soft tissue swellings ("clubbing") (Figure 5) (6).

Figure 5. Posteroanterior radiograph of hand in a patient with bronchogenic carcinoma shows periostosis along the shaft of 2nd metacarpals (white arrow).

Systemic connective tissue disorders and granulomatous conditions

Scleroderma: Scleroderma is a connective tissue disorder with typical imaging manifestations of acro-osteolysis, peri-articular osteopenia, and erosions. Subcutaneous calcifications are also seen, particularly on the extensor surfaces of the hands (Figure 6) (3).

Dermatomyositis: Dermatomyositis is an autoimmune inflammatory myopathy which causes a non-deforming arthritis with swelling of the distal joints of the hands. Radiographic features include cutaneous linear lacy reticular calcific deposits (40%) with a widespread distribution. Unlike scleroderma, osteopenia is not a feature (3).

Marfan's syndrome: Marfan's syndrome is an inherited multi-systemic connective disease demonstrating Steinberg sign (protrusion of the thumb beyond the confines of the clenched fist). A metacarpal index (averaging the four ratios of length of 2nd to 5th metacarpals divided by their respective mid-diaphyseal width) greater than 8.8 for males or 8.4 for females suggestive of arachnodactyly (Figure 7) (7).

Sarcoidosis: Sarcoidosis is a chronic granulomatous disease with 15-25% of cases featuring as oligoarthritis and symmetric poly arthritis. Usually, the proximal inter-phalangeal joints and phalanges are affected demonstrating the classical cyst like radiolucent areas with 'lacy' lytic appearance which may lead to pathological fractures and alignment deformities (Figure 8) (3).

Tuberculous dactylitis (Spina Ventosa): In India, tuberculosis is a masquerader of almost every other disease and has to be kept in mind while reviewing the radiology images. Tuberculous dactylitis involves the short tubular bones

Figure 6. Scleroderma in a 25-year-old female. Posteroanterior radiograph of right hand shows acro-osteolysis (white arrow) evident in all distal phalanges. Multiple soft tissue calcifications (yellow arrow) are also seen.

Figure 7. Marfans syndrome in a 30-year-old female. Posteroanterior radiograph of both hands shows elongation of the phalanges.

of hands and feet. The proximal phalanx of the index and middle fingers and the metacarpals of the middle and ring fingers are the most common sites involved, presenting as soft tissue swelling and periostitis. Fusiform swelling of the bone with thinned cortex and a radiolucent marrow space is characteristic, eventually resulting in cortical destruction and soft tissue swelling. A cyst-like cavity with ballooning out of the bone gives the appearance termed 'spina ventosa' ("wind-filled sail") (Figure 9) (8).

Figure 8. Sarcoidosis in a 44-year-old man. Posteroanterior radiograph of left hand shows extensive lytic lesions involving the phalanges with lacy lytic appearance & acro-osteolysis of distal phalanges.

Endocrine and metabolic disorders

Thyroid acropachy: Acropachy occurs as one of the extra-thyroid manifestations of Grave's disease, clinically presenting as painless swelling of the hands and feet. Hand radiograph shows bilateral, symmetric thick, spiculated (feathery), and periosteal reactions. Conversely, the periostitis seen in hypertrophic osteoarthropathy is smoothly layered and usually tender (3).

Acromegaly: Acromegaly is the result of excessive growth hormone production, most commonly from pituitary macroadenoma. Radiographs reveal osseous enlargement and widening of the terminal phalangeal tufts, giving a spade-like appearance. Other features may include widened joint spaces (Figure 10). Generalized osteoporosis and premature osteoarthritis are also described (3).

Hypothyroidism: Congenital hypothyroidism causes severe skeletal deformities and delays in development. Acquired hypothyroidism, on the other hand, causes only minor, if any, skeletal abnormalities. Children's radiographs show uneven epiphyseal ossification and delayed carpal bone ossification. Also possible is a delay in dental development (9).

Figure 9. Tuberculous dactylitis in a 28-year-old male with prior history of pulmonary tuberculosis. Posteroanterior radiograph of the right hand shows a thinned cortex surrounding a lytic lesion with trabecular pattern involving the proximal third metacarpal (white arrow).

Figure 10. Posteroanterior radiograph of both hands in a patient with pituitary macroadenoma shows widening of the terminal phalangeal tufts (white arrow) with prominent soft tissue structures.

Hyperparathyroidism: When parathyroid hormone is produced uncontrollably, hyperparathyroidism raises calcium and alkaline phosphatase levels in the blood while lowering phosphate levels. It can be either primary or secondary (commonly due to chronic renal insufficiency). Osteopenia and bone demineralization are frequently visible on hand radiographs. The radial aspect of the proximal and middle phalanges of the second and third digits have subperiosteal bone resorption, which is the pathognomonic finding. Initial research indicates proximal metaphyseal cortical abnormality. Brown tumors, acro-osteolysis, and cortical resorption are examples of chronic characteristics (Figure 11) (9).

Hypoparathyroidism: Hypoparathyroidism occurs due to the reduction in parathyroid hormone resulting in reduced calcium and increased phosphate levels. Radiograph shows osteosclerosis, dense metaphyseal bands, and subcutaneous calcification (10).

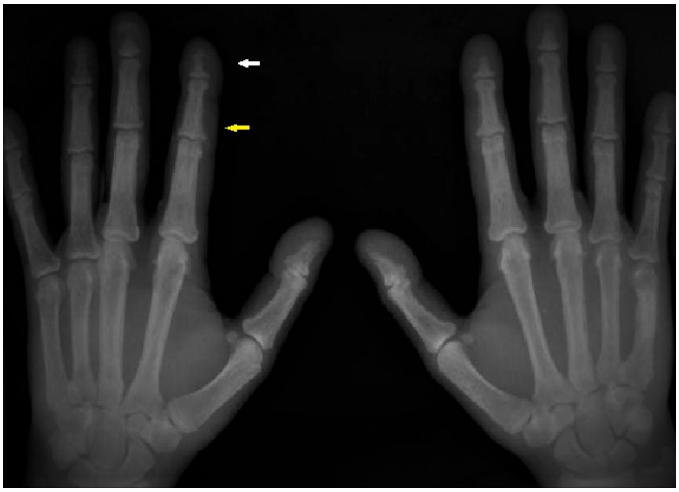

Figure 11. Chronic renal insufficiency and secondary hyperparathyroidism in a 50-year-old man. Posteroanterior radiograph shows subperiosteal bone resorption (yellow arrow) along the radial aspect of the middle phalanges of 2nd, 3rd, 4th and 5th digits with acro-osteolysis (white arrow).

Pseudohypoparathyroidism: Genetic abnormality with defect in parathyroid hormone receptor resulting in end-organ resistance to parathyroid hormone. Most striking radiographic features include brachydactyly of the metacarpal and metatarsal bones. Shortening of metacarpals (symmetric or asymmetric) with descending order of frequency: 4th, 5th, 3rd, 1st , and 2nd. Epiphyseal anomalies include premature epiphyseal fusion of the tubular bones and cone-shaped epiphyses (Figure 12) (11).

Pseudo-pseudohypoparathyroidism: Pseudo-pseudohypoparathyroidism is a genetic abnormality with radiograph features of pseudohypoparathyroidism and normal blood levels of parathyroid hormone, calcium and phosphate (11).

Haemochromatosis: Haemochromatosis is an iron overload disorder characterized by the pathological deposition of iron in tissues eventually resulting in dysfunction. Radiographic features include uniform symmetric joint space narrowing, particularly of the metacarpophalangeal joints without causing erosions. Hook-like osteophytes on the radial aspect of the metacarpal heads (especially the second) are characteristic. Chondrocalcinosis within the triangular cartilage of the wrist is seen in up to 50% of cases (11).

Figure 12. Pseudo hypoparathyroidism in a 13-year-old male with short stature and developmental delay. Posteroanterior radiograph shows short left 4th metacarpal bone (white arrow) and cone-shaped epiphyses of distal phalanx of both thumbs.

Rickets: Rickets is characterized by deficient mineralization of the growth plates of growing children, the most frequent cause is nutritional deficiency of vitamin D. Radiographic findings are seen in the metaphyses of the fastest growing bones including the distal radius and ulna, distal femur, proximal and distal tibia, proximal humerus and the anterior ends of the middle ribs, which include axial widening of the growth plate, loss of the zone of provisional calcification, cupping, splaying, and fraying of the metaphyses (Figure 13) (12,13).

Osteoporosis: Osteoporosis is characterized by diminished bone mass and skeletal fragility. More than 30-50% bone loss should be present to appreciate the decreased density on a radiograph. Most attributed causes are postmenopausal status and old age. Vertebrae, proximal femur, tubular bones, and calcaneum are analyzed to assess the bone loss. Hand radiograph shows thinning of the cortex of the tubular bones, with a cortical thickness of <25 percent of the whole thickness of metacarpal signifying osteoporosis (9).

Renal Osteodystrophy: Renal osteodystrophy refers to the complex of musculoskeletal abnormalities observed in the setting of chronic renal insufficiency. Radiographic findings include those of osteo¬malacia and secondary hyperparathyroidism (9).

Figure 13. Rickets in a twelve-year-old boy. Posteroanterior radiograph shows cupping, splaying, and fraying of the metaphysis of distal radius and ulna.

Hematological disorders

Sickle cell disease: Sickle cell disease is an inherited (autosomal recessive) disorder that causes the development of aberrant haemoglobin (a hemoglobinopathy), which causes hemolytic anaemia and multisystem ischemia and infarction. Sickle cell hand foot syndrome includes diaphyseal lytic lesions, periostitis and soft tissue swelling within the tubular bones of the hands and feet (14).

Thalassemia: Thalassemia is an autosomal recessive hemoglobinopathy with its roots in the Mediterranean belt. Imaging findings include coarsening of trabecular pattern and expansion of the metacarpal shafts. Bone maturation is retarded with delayed epiphyseal fusion of hand bones. Nutrient foramina often appear large (Figure 14) (15).

Fanconi's Anemia: Fanconi anaemia is an autosomal recessive condition marked by increasing bone marrow failure, a number of congenital anomalies, and a propensity for malignancies (often acute myeloid leukemia). It is thought to be the most typical variety of hereditary marrow failure syndrome. Imaging features include aplasia or hypoplasia of the bones of thumb, 1st metacarpal and radius. (Figure 15) (16).

Leukemia: Even though bone marrow infiltration is the leukemia's primary defining feature, involvement of the musculoskeletal system is not usually visible on imaging. Radiolucent metaphyseal bands are the most frequent finding. Lytic lesions in the diaphysis of long bones giving a "moth eaten appearance." Osteopenia and periosteal reactions are the other imaging manifestations (17).

Skeletal dysplasias

Many skeletal dysplasias include acral manifestations. In this pictorial review we have highlighted some of the important and common entities.

Figure 14. Thalassaemia in a 25-year-old man. Posteroanterior radiograph shows coarsening of trabecular pattern with periosteal reaction along shafts of proximal phalanges of 2nd, 3rd, and 4th digits.

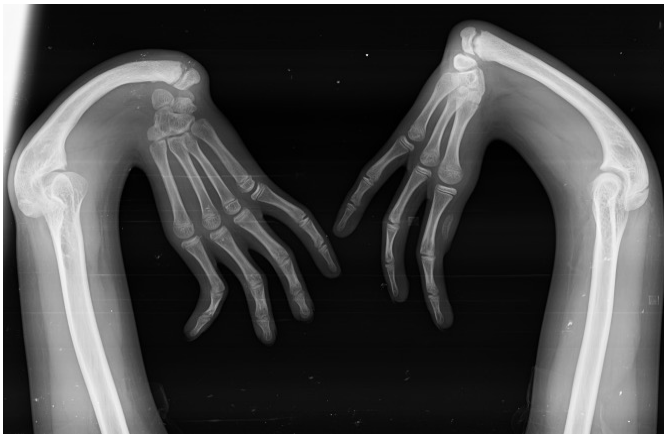

Figure 15. Fanconi's anemia in a nine-year-old male with deformed arms. Posteroanterior radiograph of both hands shows aplasia of bones of thumb and radius of both hands and aplasia of bones of right index finger and carpals. Left carpal fusion noted.

Mucopolysaccharidosis: Mucopolysaccharidosis (MPS) are a group of lysosomal storage disorders due to deficiency of lysosomal enzymes necessary to break down mucopolysaccharides. Radiographs of the hands may show a characteristic pointing or tapering of the proximal portion of the metacarpals with bullet shaped appearance. Hypoplastic and irregular carpal bones are seen (Figure 16). V shaped appearance of the hypoplastic distal ulna and radius (18).

Achondroplasia: Rhizomelic dwarfism, large head with frontal bossing, hypoplasia of the midface and trident hands are the characteristic features in achondroplasia. On hand radiograph, the hand is trident shaped with short stubby fingers and separation is seen between the middle and ring fingers (Figure 17). Associated thumb hypoplasia is also seen (18).

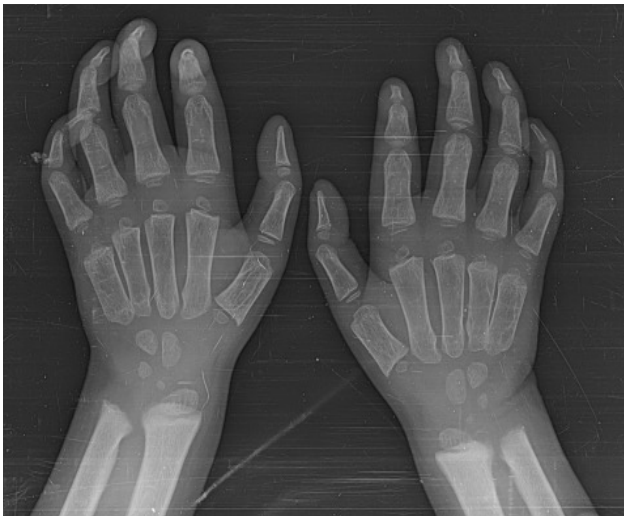

Figure 16. Five-year-old male with mucopolysaccharidosis. Posteroanterior radiograph shows tapering of the proximal portion of the metacarpals with bullet shaped appearance.

Figure 17. Achondroplasia in a three-year-old male. Posteroanterior radiograph shows trident shaped hand with separation between middle and ring fingers.

Pyknodysostosis: Pyknodysotosis is characterized by osteosclerosis, short limb dwarfism, and skeletal fragility. Hands and feet are short and stubby, with partial aplasia of the terminal phalanges (acro-osteolysis) (Figure 18). There is preservation of medullary canal in contrast to osteopetrosis (18).

Osteopetrosis: Osteopetrosis is characterized by lack of resorption of normal primitive osteochondrous tissue. Patients have brittle, dense bones and are subjected to multiple pathological fractures. On radiograph there is increased density of the skeleton with no cortico-medullary differentiation. Striations produce bone within a bone appearance/endobones typically noted in short tubular bones, spine, and pelvis (Figure 19) (18).

Figure 18. Pyknodysostosis in a fifteen-year-old female with short stature. Posteroanterior radiograph shows generalized increase in bone density with preservation of medullary canal and acroosteolysis.

Figure 19. Osteopetrosis in a seven-year-old male. Posteroanterior radiograph shows generalized increased density of bones with no cortico-medullary differentiation and bone within a bone appearance: endo-bones.

Conclusion

Abnormalities of the hands may provide a clue to the diagnosis of various systemic diseases. The predisposition of certain joints along with characteristic features will help in arriving at a diagnosis of the underlying systemic disorder. It is essential for the radiologists to be aware of the acral manifestations of systemic disorders to aid in diagnosis and treatment.

References

1. Glasser O. W. C. Roentgen and the discovery of the Roentgen rays. AJR Am J Roentgenol. 1995 Nov;165(5):1033-40. doi: https://doi.org/10.2214/ajr.165.5.7572472. PMID: 7572472.

2. Jacobson JA, Girish G, Jiang Y, Sabb BJ. Radiographic evaluation of arthritis: degenerative joint disease and variations. Radiology. 2008 Sep;248(3):737-47. doi: https://doi.org/10.1148/radiol.2483062112. PMID: 18710973.

3. Jacobson JA, Girish G, Jiang Y, Resnick D. Radiographic evaluation of arthritis: inflammatory conditions. Radiology. 2008 Aug;248(2):378-89. doi: 10.1148/radiol.2482062110. PMID: 18641245.

4. Miksanek J, Rosenthal AK. Imaging of calcium pyrophosphate deposition disease. Curr Rheumatol Rep. 2015 Mar;17(3):20. doi: 10.1007/s11926-015-0496-1. PMID: 25761927; PMCID: PMC5471493.

5. Omoumi P, Zufferey P, Malghem J, So A. Imaging in Gout and Other Crystal-Related Arthropathies. Rheum Dis Clin North Am. 2016 Nov;42(4):621-644. doi: 10.1016/j.rdc.2016.07.005. Epub 2016 Sep 9. PMID: 27742018.

6. Yap FY, Skalski MR, Patel DB, Schein AJ, White EA, Tomasian A, Masih S, Matcuk GR Jr. Hypertrophic Osteoarthropathy: Clinical and Imaging Features. Radiographics. 2017 Jan-Feb;37(1):157-195. doi: 10.1148/rg.2017160052. Epub 2016 Dec 9. PMID: 27935768.

7. Giampietro PF, Raggio C, Davis JG. Marfan syndrome: orthopedic and genetic review. Curr Opin Pediatr. 2002 Feb;14(1):35-41. doi: 10.1097/00008480-200202000-00006. Erratum in: Curr Opin Pediatr 2002 Apr;14(2):286. PMID: 11880731.

8. Abebe W, Abebe B, Molla K, Alemayehu T. Tuberculous Dactylitis: An Uncommon Presentation of Skeletal Tuberculosis. Ethiop J Health Sci. 2016 May;26(3):301-3. doi: 10.4314/ejhs.v26i3.15. PMID: 27358553; PMCID: PMC4913200.

9. Chang CY, Rosenthal DI, Mitchell DM, Handa A, Kattapuram SV, Huang AJ. Imaging Findings of Metabolic Bone Disease. Radiographics. 2016 Oct;36(6):1871-1887. doi: 10.1148/rg.2016160004. PMID: 27726750.

10. Veena C, Kumar GA, Niranjan K. Diagnostic Radiology: Musculoskeletal and Breast Imaging (Aiims-Mamc-Pgi Imaging). Jaypee Brothers Medical Publishers (p) Ltd. ISBN:B00FF5VQ94.

11. Resnick D, Kransdorf MJ. Bone and joint imaging. Third edition. Pennysylvania: Elsevier ; 2005. 619 p.

12. Shore RM, Chesney RW. Rickets: Part I. Pediatr Radiol. 2013 Jan;43(2):140-51. doi: 10.1007/s00247-012-2532-x. Epub 2012 Dec 1. PMID: 23208530.

13. Shore RM, Chesney RW. Rickets: Part II. Pediatr Radiol. 2013 Jan;43(2):152-72. doi: 10.1007/s00247-012-2536-6. Epub 2012 Nov 21. PMID: 23179485.

14. Ejindu VC, Hine AL, Mashayekhi M, Shorvon PJ, Misra RR. Musculoskeletal manifestations of sickle cell disease. Radiographics. 2007 Jul-Aug;27(4):1005-21. doi: 10.1148/rg.274065142. PMID: 17620464.

15. Gosein M, Maharaj P, Balkaransingh P, Banfield R, Greene C, Latchman S, Sinanan A. Imaging features of thalassaemia. Br J Radiol. 2019 Mar;92(1095):20180658. doi: 10.1259/bjr.20180658. Epub 2018 Nov 14. PMID: 30412423; PMCID: PMC6540857.

16. De Kerviler E, Guermazi A, Zagdanski AM, Gluckman E, Frija J. The clinical and radiological features of Fanconi's anaemia. Clin Radiol. 2000 May;55(5):340-5. doi: 10.1053/crad.2000.0445. PMID: 10816398.

17. Riqulme VS, Garcia CV .Imaging studies in early diagnosis of childhood leukaemia. Rev Chil Radiol. 2012; 18 (1): 24–29.

18. Panda A, Gamanagatti S, Jana M, Gupta AK. Skeletal dysplasias: A radiographic approach and review of common non-lethal skeletal dysplasias. World J Radiol. 2014 Oct 28;6(10):808-25. doi: 10.4329/wjr.v6.i10.808. PMID: 25349664; PMCID: PMC4209426.